Self-affine nature of the stress-strain behavior of thin fiber networks

Alexander S. Balankin,[1,*] Orlando Susarrey,[1] and Armando Bravo[2]
[1]*SEPI-ESIME, Edificio 5, 3er Piso, Instituto Politécnico Nacional, Mexico, Distrito Federal 07738, Mexico*
[2]*Instituto Tecnológico y de Estudios Superiores de Monterrey, Campus Estado de México, Mexico, 52926 Mexico*
(Received 27 May 2001; published 27 November 2001)

The stress-strain behavior of toilet paper is studied. We find that the damaged parts of stress-strain curves possess a self-affine scaling invariance. Moreover, we find that the stress-strain behavior and the rupture line roughness are characterized by the same scaling (Hurst) exponent H, which is not universal: rather it changes from sample to sample. The variations on H are mainly due to fluctuations in the paper structure, which are larger than statistical errors within a sample. Furthermore, the same exponent governs the changes in the stress-strain curve as the strain rate increases. The fractal damage model is employed to explain experimental observations.

DOI: 10.1103/PhysRevE.64.066131 PACS number(s): 46.50.+a, 05.40.−a, 47.53.+n, 61.43.Hv

Fiber networks form a class of materials in which disorder plays an important role in mechanical behavior [1–3]. Whether the material in question is paper, a glass fiber mat, or a stochastically oriented fiber composite, the local stress varies widely due to local density variations and fluctuations in the local stress transfer [1]. These fluctuations are manifested in the stochastic nature of rupture lines. It was found that crack traces in solids are not at random, instead they possess self-affine invariance, characterized by a well-defined crack roughness (Hurst) exponent H [4–7]. That is, if a crack trace is represented by a single-valued function $z(x)$, then $z(\lambda x) \cong \lambda^H z(x)$ for any $\lambda > 0$, where "$\cong$" denotes equality in a statistical sense. Crack traces in a paper possess a statistical self-affine invariance within a wide but bounded range of scale length, $\ell_0 < x < \xi_c$, where the lower, ℓ_0, and the upper, ξ_c, cutoffs are determined by the paper structure [8]. Generally, scaling properties of rough interfaces (specifically cracks) are more complex [5,9,10].

Instead of a single crack growth, the failure of fiber networks may also occur as the culmination of progressive damage, involving complex interactions between multiple defects and growing microcracks [1,3,7,11]. In such a case, the stress-strain curve shows a stochastic nature. This fracture behavior is characteristic of many disordered fibrous materials, such as fiber-reinforced composites and various kinds of paper [1,7]. The interaction between multiple defects and several characteristic scales present a considerable challenge to the modeling and prediction of rupture.

In this work, we study the failure of toilet paper under uniaxial tensile loading. The paper can be treated as a quasi-planar network with an asymmetrically orientated distribution of fibers [2]. The fiber distribution is not random, but possesses long-range mass density correlations of a power-law type [12]. The latter indicates the (multi-) fractal nature of the paper structure [13]. The thickness and areal density of the toilet paper display considerable variations in accordance with a normal distribution with means $h = 0.11 \pm 0.06$ mm and $\rho = 36.8 \pm 0.3$ g/m^2, respectively.

Several mechanical tests were carried out on a 4505 INSTRON testing machine. The deformation rate was controlled by grip displacement speeds (du/dt) of 0.5, 1, 2.5, 5, 10, and 100 mm/min, respectively. The stress-strain measurement rate was 50 points/sec. Toilet paper possesses anisotropic mechanical properties associated with a preferred fiber orientation in the machine direction. In this work, we employed paper sheets of length $L = 10$ cm and width $W = 5$ cm, which were loaded in the machine direction of paper. At least 30 paper sheets were tested for each displacement speed (deformation rate $\dot{\varepsilon} = L^{-1} du/dt = 0.005$, 0.01, 0.025, 0.05, 0.1, and 1 min^{-1}, respectively).

Toilet paper possesses a linear elastic behavior up to the tensile stress σ_M [see Fig. 1(a)]. This indicates that an individual fiber is linearly elastic up to its rupture threshold. However, different fibers achieve rupture thresholds at dif-

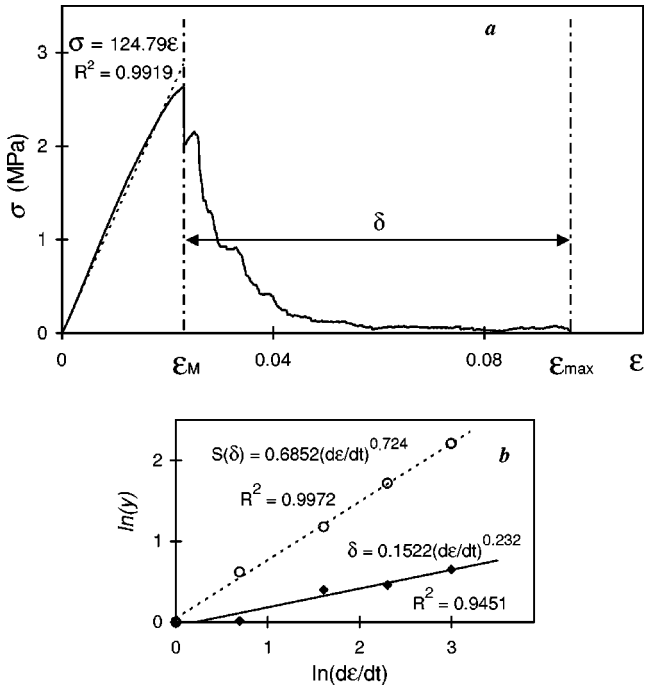

FIG. 1. (a) Engineering strain-stress curve and (b) graphs of δ and $S(\delta)$ versus strain rate for toilet paper.

*Email addresses: balankin@iris.esimez.ipn.mx and balankin@hotmail.com

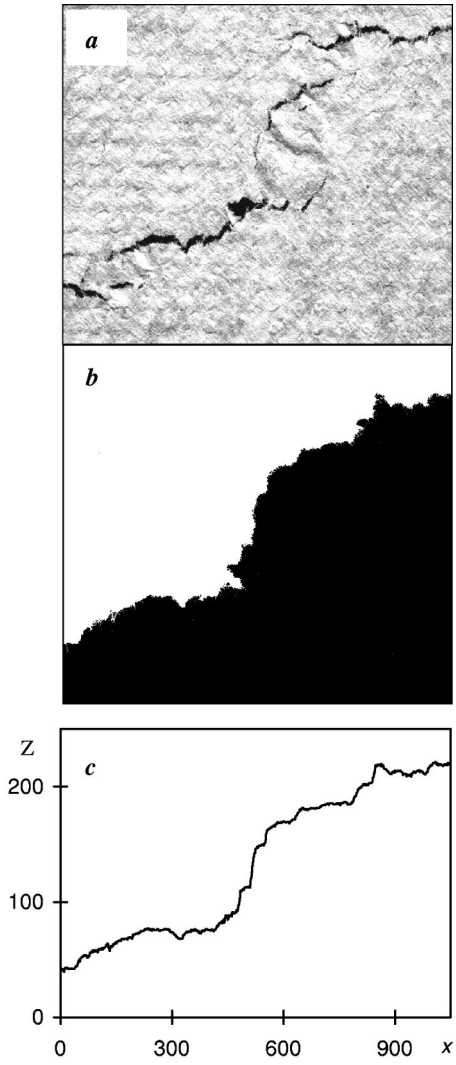

FIG. 2. (a) Damage and (b) rupture line images for toilet paper, and (c) graph of rupture line.

ferent deformations; hence, the network failure represents a progressive damage from multiple microcracks [see Fig. 2(a)]. As a result the engineering stress-strain curve displays a stochastic behavior [see Fig. 1(a)]. In the very final stage, the process of coalescence of individual microcracks gives rise to a single rupture line [see Fig. 2(b)].

It was also observed that all the stress-strain curve parameters (Young modulus E, tensile strength σ_M, deformation threshold ε_M, maximum deformation $\varepsilon_{\max}$, and deformation range of damage $\delta=\varepsilon_{\max}-\varepsilon_M$) vary from sample to sample, following a normal distribution. The means and standard deviations (S) for these distributions are functions of the strain deformation rate $\dot{\varepsilon}$ [see, for example, Fig. 1(b)]. Specifically, we find that

$$E=245\dot{\varepsilon}^{0.087}\ \text{MPa},\quad \sigma_M=2.89\dot{\varepsilon}^{0.0085}\ \text{MPa},$$

$$\varepsilon_M=0.0171\dot{\varepsilon}^{-0.0661},\quad \varepsilon_{\max}=0.16\dot{\varepsilon}^{0.17},$$

$$\delta=0.1522\dot{\varepsilon}^{0.2321},\quad S(\delta)=0.6852\dot{\varepsilon}^{0.7242}, \tag{1}$$

in the range $0.005\leqslant\dot{\varepsilon}\leqslant0.1\ \text{min}^{-1}$. These relations fail when the strain rate is $\dot{\varepsilon}=1\ \text{min}^{-1}$. The reason for this change may be the change in the failure regime [14], which will be studied in a future work.

The scaling properties of decreasing parts $(\varepsilon_M,\varepsilon_{\max})$ of stress-strain curves [Fig. 1(a)] and rupture lines [Fig. 2(b)] were studied with the use of the BENOIT 1.2 software [15]. For this purpose the fractured sheets were scanned in black and white BMP format [see Fig. 2(b)] with a 600 dpi resolution. Then the rupture lines were plotted using the Scion Image software [16] as single-valued functions $z(x)$ in the Excel (XLS) format [see Fig. 2(c)].

The scaling (Hurst) exponent of each rupture line, $z(x)$, as well as of each stress-strain curve, $\sigma(\varepsilon)$, was determined by five different statistical methods adopted in the BENOIT 1.2 software [15]: variogram, roughness-length, wavelets, power-spectrum, and rescaled-range (R/S) analysis. Specifically, for a self-affine curve, the averaged value of the squared difference between pairs of points at a distance Δ (variogram) scales with Δ as $V\propto\Delta^{2H}$, the root-mean-square roughness scales as $s\propto\Delta^H$, where s is the standard deviation, and consequently, $R/S\propto\Delta^H$, where R is the range taken by the value z in the range Δ and S is the standard deviation of the first difference of z within the interval Δ. The structure factor or power spectrum of self-affine curves scale as $P\propto q^{\beta}$, where q is the wave vector and $\beta=1+2H$. The wavelet method is based on the property that the wavelet transform of a self-affine curve has self-affine properties [15].

Figures 3(a)–3(d) show the fractal graphs obtained by the aforementioned methods for the stress-strain curve (1) and its corresponding rupture line (2) in toilet paper. The data presented in Fig. 3 suggests that the engineering stress-strain curve possesses a self-affine invariance, i.e.,

$$\sigma(\lambda\varepsilon)=\lambda^{-\alpha}\sigma(\varepsilon),\quad \text{with}\ \ \alpha=H, \tag{2}$$

where H is the rupture line roughness (Hurst) exponent, $\lambda>0$ is a constant, and $\varepsilon_M<\varepsilon$, $\lambda\varepsilon<\varepsilon_{\max}$.

From the experimental data we note that the five aforementioned methods lead to the same value of the roughness exponent $\alpha=H$ for the stress-strain curve and the corresponding rupture line [Fig. 4(a)]. At the same time, we find that the scaling exponent is not universal; rather it changes from sample to sample in accordance with a normal distribution [Fig. 4(c) and Fig. 4(d)]. These variations are larger than statistical errors within a sample and they might be attributed to the sample-to-sample variation in the network structure. On the other hand, we note that the mean value of $\alpha=H$ does not depend on the strain rate [see Fig. 4(b)].

The observed failure behavior of the toilet paper may be understood on the basis of a fractal damage model of the fiber network. Namely, the elastic energy function of a network formed by N elastic fibers can be represented as $U=0.5E(N)\varepsilon^2$, where $E(N)=E_0N(\varepsilon)$ is the elastic modulus of the network, E_0 is the fiber elastic modulus, and N is a strictly decreasing continuous function of strain ε (N decreases every time as one fiber fails). The function $N(\varepsilon)$ obeys the following properties: $N(\varepsilon\leqslant\varepsilon_1<\varepsilon_M)=N_0$, $N(\varepsilon_{\max})=0$; furthermore, $dN/d\varepsilon\cong0$, where the symbol "$\cong$"

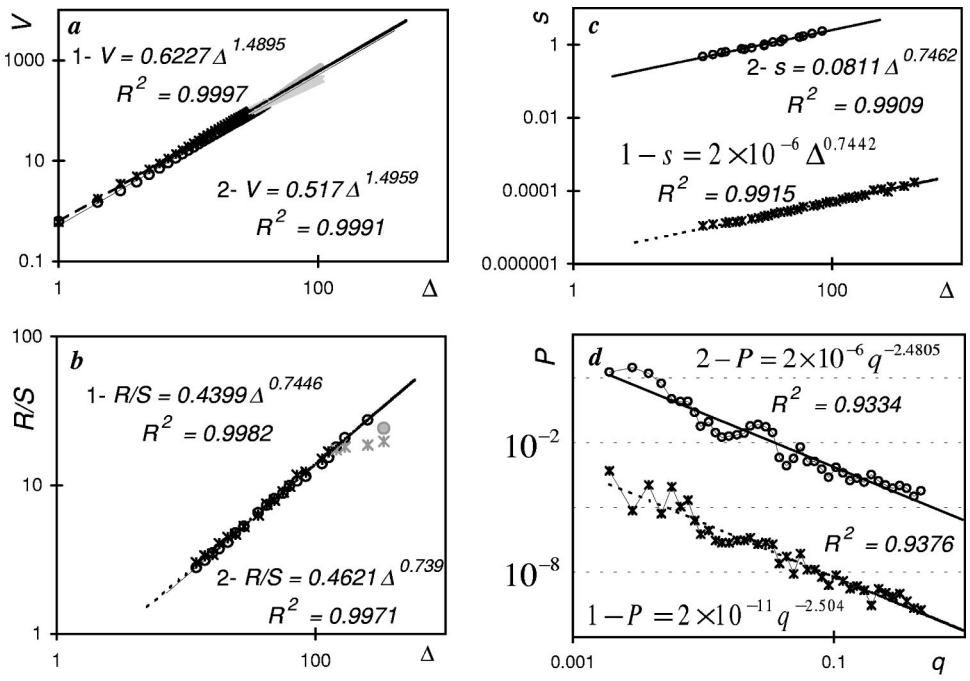

FIG. 3. Fractal graphs of the stress-strain curve (1), and corresponding rupture line (2) for toilet paper [see Figs. 1(a) and 2(b)] obtained by: (a) the variogram, (b) the roughness-length, (c) the rescaled range, and (d) the power-spectrum methods.

denotes ''equal with exception of a Lebesgue set of zero measure,'' and $dN/d\varepsilon=\infty$, when $\varepsilon=\varepsilon_i$, $i=1,2,...,N$, where ε_i is the failure strain of the ith fiber, which is a function of the strain rate [see Eq. (1)]. The simplest stepwise function that satisfies these conditions is

$$N(\varepsilon_i<\varepsilon<\varepsilon_{i+1})=\text{const}, \quad N(\varepsilon_i)=N_0[1-(\varepsilon_i/\varepsilon_{\max})],$$

$$0<\varepsilon_1\leqslant\varepsilon_2\leqslant\cdots<\varepsilon_N=\varepsilon_{\max}.$$

In this way, a fractal elastic network $N(\varepsilon>\varepsilon_1)$ can be represented by the Devil's staircase [5] associated with the Cantor set (ε_i) of fractal dimension D_C. The latter is determined by the fractal dimension of the damaged ensemble D, which is related to the fractal dimension of the fiber network, $2<D_N\leqslant 3$ [13]. Under these assumptions, $N(\varepsilon)$ possesses a statistical self-affine invariance, i.e.,

$$N(\lambda\varepsilon)=\lambda^{-\eta}N(\varepsilon), \quad \text{where } \lambda>0,$$

$$\varepsilon_1<\varepsilon, \quad \lambda\varepsilon<\delta_{\max} \quad \text{and} \quad \eta>0.$$

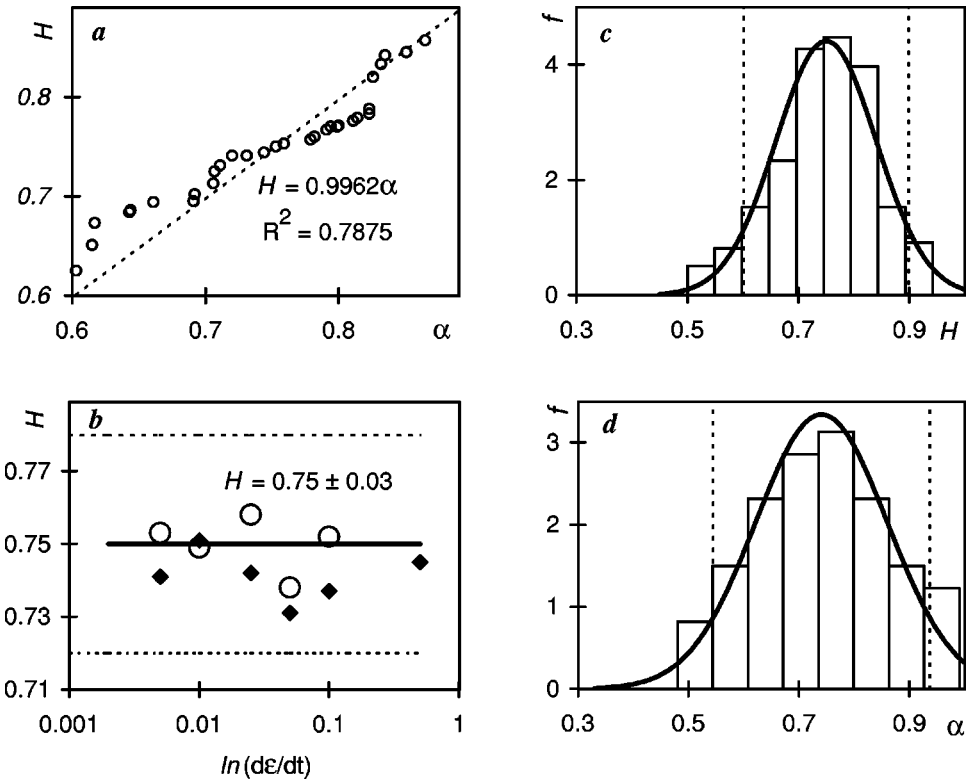

FIG. 4. (a) Graph of H versus α, for tests with a deformation rate $\dot{\varepsilon}=0.01\ \text{min}^{-1}$, (b) the mean values of H (circles) and α (rhombuses) versus strain rate, and statistical distributions of (c) α (bars—experimental data, solid line—fitting by normal distribution: significance level according to the χ^2 test with fitness $p=0.9361$), and (d) H (bars—experimental data, solid line—fitting by normal distribution: $p=0.7622$).

Using the properties of the Devil's staircase [5] and some conventional thermodynamic assumptions [17] it is easy to derive the constitutive equation for an elastic (multi-) fractal network

$$\sigma = \frac{\partial U}{\partial \varepsilon} \cong E(N(\varepsilon))\varepsilon = E_0 N(\varepsilon)\varepsilon \propto \sigma^{-\alpha},$$

which obeys a self-affine scaling (2) with $\alpha = \eta - 1$, within the interval $\varepsilon_1 < \varepsilon$, $\lambda\varepsilon < \varepsilon_{\max}$. On the other hand, under the assumption that the rupture fractal dimension D_R relates to the fractal dimension of the damaged ensemble as $D_R = D - 1$ [5,7], we have $0 < H = 2 - D_R = 3 - D \leqslant 1$. Taking into account the second equality of Eq. (2), we obtain $1 < \eta = H + 1 = 4 - D < 2$.

Furthermore, we speculate that Eq. (1) may be cast in the form

$$\delta = 0.1454\dot{\varepsilon}^{1-H}, \quad S(\delta) = 0.6852\dot{\varepsilon}^{H}, \tag{3}$$

i.e., the failure dynamics is governed by the same Hurst exponent, which depends on the network structure (see also Refs. [8,13]). To verify this assumption, a set of experiments at each deformation rate was divided in two subsets, associated with specimens with the lowest and the highest values of H. So, we obtained two sets of data with different means $H = \alpha = 0.645 \pm 0.04$ and $H = \alpha = 0.848 \pm 0.06$, respectively. For these sets, the means and standard deviations of δ scale as

$$\delta \propto \varepsilon^{0.367}, \quad SD(\delta) \propto \varepsilon^{0.639}$$

$$\text{and} \quad \delta \propto \varepsilon^{0.157}, \quad S(\delta) \propto \varepsilon^{0.841}, \tag{4}$$

respectively. One can see that relations (1) are in a good agreement with Eq. (3).

From Eq. (3), it follows that for a smooth ($H = 1$) rupture line, one may expect $\delta = \text{const}$, and $SD(\delta) \propto \dot{\varepsilon}$, while for a random ($H = 0.5$) damage, $\delta \propto S(\delta) \propto \dot{\varepsilon}^{0.5}$. A further study on different materials, including the fractal analysis of the network structure, is needed in order to confirm the general character of the fractal failure behavior shown in Eqs. (2), (3).

This work was supported by the Mexican Government under the CONACyT Grant No. 34951-U and by the Mexican Oil Institute under the Pipeline Integrity Program.

[1] *Statistical Models for the Fracture of Disordered Media*, edited by H. J. Herrmann and S. Roux (North-Holland, Amsterdam, 1990); B. H. Kaye, *A Random Walk Through Fractal Dimensions*, 2nd ed. (VCH Publishers, New York, 1994).

[2] M. Deng and C. T. J. Dodson, *Paper: An Engineering Stochastic Structure* (Tappi Press, Atlanta, 1994).

[3] J. A. Aström and K. J. Niskanen, Europhys. Lett. **21**, 557 (1993); A. S. Balankin and P. Tamayo, Rev. Mex. Fis. **40**, 506 (1994); V. I. Räisänen, M. J. Alava, and R. M. Nieminen, J. Appl. Phys. **82**, 3747 (1997).

[4] B. Mandelbrot, *The Fractal Geometry of Nature* (Freedom, New York, 1988); P. Meakin, *Fractals, Scaling and Growth far From Equilibrium* (Cambridge University Press, New York, 1998).

[5] A.-L. Barabási and H. E. Stanley, *Fractal Concepts in Surface Growth* (Cambridge University Press, Cambridge, 1995).

[6] K. J. Maloy *et al.*, Phys. Rev. Lett. **68**, 213 (1992); J.-P. Bouchaud *et al.*, *ibid.* **71**, 2240 (1993); J. Schmittbuhi *et al.*, *ibid.* **74**, 1787 (1995); P. Daguier, *ibid.* **78**, 1062 (1997).

[7] G. P. Cherepanov, A. S. Balankin, and V. S. Ivanova, Eng. Fract. Mech. **51**, 997 (1995); A. S. Balankin, and F. Sandoval, Rev. Mex. Fis. **43**, 545 (1997); A. S. Balankin, Eng. Fract. Mech. **57**, 135 (1997), and references therein.

[8] A. S. Balankin and O. Susarrey, Int. J. Fract. **81**, R27 (1996); A. S. Balankin *et al.*, *ibid.* **87**, L37 (1997); *ibid.* **90**, L57 (1998); A. S. Balankin and O. Susarrey, Philos. Mag. Lett. **79**, 629 (1999).

[9] J. M. Lopez, Phys. Rev. Lett. **83**, 4594 (1999); J. J. Ramasco, *ibid.* **84**, 2199 (2000).

[10] A. S. Balankin, D. Morales, and I. Campos, Philos. Mag. Lett. **80**, 165 (2000).

[11] A. Mosolov, Chaos, Solitons Fractals **4**, 2093 (1994); G. S. Bhattacharya and B. K. Raghuprasad, Int. J. Fract. **82**, R73 (1996).

[12] N. Provatas, M. J. Alava, and T. Ala-Nissila, Phys. Rev. E **54**, R36 (1996).

[13] A. S. Balankin *et al.*, Proc. R. Soc. London, Ser. A **455**, 2565 (1999); A. S. Balankin, A. Bravo, and D. Morales, Philos. Mag. Lett. **80**, 503 (2000).

[14] I. L. Menezes-Sobrino, J. G. Moreira, and A. T. Bernardes, Eur. Phys. J. B **13**, 313 (2000).

[15] http://www.trusoft-international.com (BENOIT 1.2, 1999); W. Seffens, Science **285**, 1228 (1999).

[16] http://www.sciocorp.com (Scion Image, 1999).

[17] L. D. Landau and E. M. Lifshitz, *The Theory of Elasticity*, 3rd ed. (Butterworth-Heinemann, Oxford, 1986).